Inorganic Chemistry
Article

Inorg. Chem. **2009**, *48*, 8415–8422 **8415**
DOI: 10.1021/ic901014r

Cationic Dimetallic Gold Hydride Complex Stabilized by a Xantphos-Phosphole ligand: Synthesis, X-ray Crystal Structure, and Density Functional Theory Study

Aurélie Escalle,[†] Guilhem Mora,[†] Fabien Gagosz,[‡] Nicolas Mézailles,[†] Xavier F. Le Goff,[†] Yves Jean,[*,†] and Pascal Le Floch[*,†]

[†]*Laboratoire "Hétéroéléments et Coordination", and* [‡]*Laboratoire de Synthèse Organique, Ecole Polytechnique, CNRS, 91128 Palaiseau Cedex, France*

Received May 26, 2009

The bis-2,5-diphenylphosphole xantphos ligand (XDPP) **1** reacts with the [AuCl(tht)] complex to afford the monocoordinated [Au(XDPP)Cl] **2** and the dicoordinated chelate species [Au(XDPP)Cl] **3**. Addition of AgOTf on this mixture, at room temperature, affords the cationic [Au(XDPP)][OTf] complex **4** which was fully characterized. An X-ray crystal structure analysis confirms the bent structure of this 14 VE $[ML_2]^+$ complex. Reaction of **4** with $HSiMe_2Ph$ in tetrahydrofuran at −78 °C yields the dinuclear [(XDPP)Au−H−Au(XDPP)]$^+$ cationic complex **5**, in which the hydride bridges the two [Au(XDPP)]$^+$ metal fragments. In **5**, the Au−P bond lengths are different and the phosphorus atoms which are located nearly trans to the hydride ligand exhibit significantly shorter P−Au bond lengths. Reaction of **4** with $DSiMe_2Ph$ to form the [(XDPP)Au-D-Au(XDPP)]$^+$complex **6** allowed to unambiguously ascribe the chemical shift of the deuteride in ^2H NMR (δ = 7.0 ppm with a $^2J_{DP}$ = 8.4 Hz. The electronic structure of the [(XDPP)Au−H−Au(XDPP)]$^+$ complex was studied through density functional theory calculations. An orbital analysis is developed in which complex **5** is viewed as the combination of two 12 electrons fragments [Au(XDPP)]$^+$ with H^-. This analysis reveals that the hydride interacts in a bonding way with the σ MO between the two gold atoms and in an antibonding way with a combination of d orbitals at the metal centers. This simple description allows to rationalize the inequivalence of the two types of P−Au bonds in **5**.

Introduction

Phospholes, unsaturated phosphorus-containing five-membered heterocycle, exhibit a very rich chemistry that makes them very useful building blocks in phosphorus chemistry.[1] Their reactivity and properties have been extensively exploited in different contexts to elaborate new phosphorus structures such as phosphametallocenes,[2] new heterocycles, precursors of materials,[3] and so forth. Thanks to the readily modified backbone, which allows fine-tuning of the electronic properties of the phosphorus atom, they have also been widely used as ligands in homogeneous catalysis. Among these, the 2,5-diphenyl derivative is particularly attractive to elaborate robust catalysts because of its very good stability toward air oxidation. Furthermore, the precursor of these P-functional compounds, the 1,2,5-triphenylphosphole, easily available on a multigram scale from the simple condensation of dichlorophenylphosphine with 1,4-diphenyl-1,3-butadiene.[4] A few years ago, we launched a program aimed at evaluating the 2,5-diphenylphosphole (DPP) motif in catalytic transformations of synthetic relevance. Various mixed ligands such as those featuring either pyridine derivatives[5a−c] or an ancillary olefin ligand[5d] were produced and already proved to be very efficient in catalytic transformations such as hydrogen transfer processes,[5e] C−C and C−B coupling reactions,[5a−c,e] and hydroformylation.[6] Much more recently we focused our researches on a new

*To whom correspondence should be addressed. E-mail: pascal.lefloch@polytechnique.edu (P.L.F.), yves.jean@polytechnique.edu (Y.J.). Fax: +33-169334440 (P.L.F.). Phone: +33-169334401 (P.L.F).

(1) (a) Quin, L. D. *Phosphorus-Carbon Heterocyclic Chemistry: The Rise of a New Domain*; Mathey, F., Ed.; Pergamon: Amsterdam, 2001; p 219. (b) Quin, L. D. In *Phosphorus-Carbon Heterocyclic Chemistry: The Rise of a New Domain*; Mathey, F., Ed.; Pergamon: Amsterdam, 2001; p 307.

(2) (a) Mathey, F. *Coord. Chem. Rev.* **1994**, *137*, 1–52. (b) Le Floch, P. *Coord. Chem. Rev.* **2006**, *250*, 627–681.

(3) (a) Baumgartner, T.; Réau, R. *Chem. Rev.* **2006**, *106*, 4681. (b) Crassous, J.; Réau, R. *Dalton Trans.* **2008**, 6865–6876. (c) Hobbs, M. H.; Baumgartner, T. *Eur. J. Inorg. Chem.* **2007**, 3611–3628.

(4) Mora, G.; Deschamps, B.; van Zutphen, S.; Le Goff, X. F.; Ricard, L.; Le Floch, P. *Organometallics* **2007**, *26*, 1846–1855.

(5) (a) Thoumazet, C.; Melaimi, M.; Ricard, L.; Mathey, F.; Le Floch, P. *Organometallics* **2003**, *22*, 1580–1581. (b) Melaimi, M.; Thoumazet, C.; Ricard, L.; Le Floch, P. *J. Organomet. Chem.* **2004**, *689*, 2988–2994. (c) Thoumazet, C.; Melaimi, M.; Ricard, L.; Le Floch, P. *C. R. Chimie* **2004**, *7*, 823–832. (d) Thoumazet, C.; Ricard, L.; Grützmacher, H.; Le Floch, P. *Chem. Commun.* **2005**, 1592–1594. (e) Thoumazet, C.; Melaimi, M.; Ricard, L.; Mathey, F.; Le Floch, P. *Organometallics* **2003**, *22*, 1580.

(6) Mora, G.; van Zutphen, S.; Thoumazet, C.; Le Goff, X. F.; Ricard, L.; Grutzmacher, H.; Le Floch, P. *Organometallics* **2006**, *25*, 5528–5532.

(7) (a) Mora, G.; Piechaczyk, O.; Le Goff, X. F.; Le Floch, P. *Organometallics* **2008**, *27*, 2565–2569. (b) Mora, G.; van Zutphen, S.; Klemps, C.; Ricard, L.; Jean, Y.; Le Floch, P. *Inorg. Chem.* **2007**, *46*, 10365–10371.

Published on Web 08/03/2009

Scheme 1. XDPP Ligand

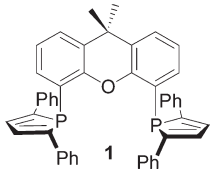

derivative (XDPP) **1** of this DPP compound featuring the Xantphos backbone (Scheme 1).[7]

This molecule proved to be a remarkable bidentate ligand for group 10 metals, and the corresponding reduced [M(XDPP)$_2$] complexes (M = Pd, Pt) were found to exhibit unusual catalytic properties. Thus, Pd(allyl) complexes such as **I** or the dimeric species **II** act as very efficient precursors of 14 VE Pd and Pt catalysts which can achieve allylation of primary arylamines (Pd)[8] and arylamines (Pt)[9] with allylalcohols under mild conditions (Scheme 2).

As part of our investigations, we recently extended our studies to cationic derivatives of group 11 metals and therein we wish to report on the case of Au(I) complexes. Our interest in the Au(I) chemistry is two-fold. First, only a few 14 VE chelated Au(I) complexes have been reported so far, and their chemistry, as well as their catalytic properties, remains largely unexplored.[10] Second, even if Au−H has been observed in the gas phase,[11] mono metallic Au−H fragments characterized from solution phase are very rare, yet phosphine−Au-H species have been postulated as catalytic intermediates.[12] In fact, when this study was undertaken, no simple [(ligand)Au−H] complex had been reported. It is clearly related to the only synthetic strategy available, namely, the reaction of a Au−Cl moiety with a hydride source. Indeed, it is well-known that [(R$_3$P)AuCl] is readily reduced to Au clusters or even phosphine stabilized Au nanoparticles by such sources. The characterization/isolation of [(R$_3$P)AuH] species was therefore a challenge. While our work was in progress, the first [L-AuH] complex was reported, with L being a NHC (N-heterocyclic carbene) ligand.[13] In the same study, the authors also isolated and structurally characterized an interesting triangular cationic gold hydride dimer **V**, isolobal of H_3^+, with a short intramolecular Au(I)−Au(I) interaction (Scheme 3). Unfortunately, no information from the Au−H bond could be retrieved since the hydride could not be structurally localized. We reasoned that the peculiar electronic and geometrical properties of our XDPP ligand (wide bite angle + acceptor properties) could allow the stabilization of the elusive "phosphine-AuH" like species, and the precise analysis of the Au−H interaction. Our results in this endeavor are presented herein.

Scheme 2. Palladium and Platinum Catalysts Used in the Allylation of Amines and Featuring the XDPP Ligand

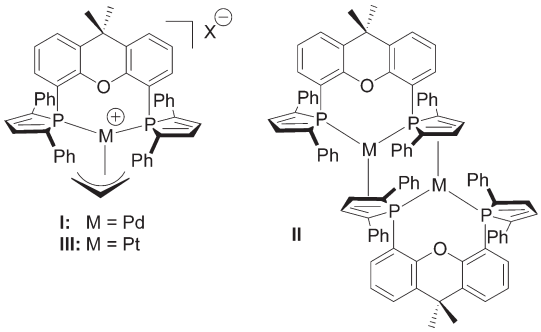

Results and Discussion

Synthesis of Complexes. In a first series of experiments, we explored the coordinating behavior of ligand **1** toward the Au(I) source [AuCl(tht)] (tht = tetrahydrothiophene). Reactions of **1** with this complex at room temperature in dichloromethane affords two complexes that are formed in a 1:1 ratio. Indeed, examination of the ^{31}P NMR spectrum of the crude mixture reveals the presence of three signals: one at 11.6 ppm and two of similar intensity at $\delta = 30.3$ ppm and $\delta = -13.3$ ppm. No attempts were made to isolate and separate these two complexes, but on the basis of these data one may propose that their complex **2** is a gold dicoordinated species (δ = 11.6 ppm) whereas complex **3** is a monocoordinated species with one pendant phosphole unit (signal at δ = 30.3 ppm, δ = −13.3 ppm for the coordinated and non-coordinated phosphorus atoms of the ligand, respectively). As a comparison, the shift of phosphorus in the free ligand **1** is −15.9 ppm. These two complexes result from the complexation of the two conformations of the free ligand **1** which are in equilibrium at room temperature.[14] Addition of 1 equiv of a chloride abstractor (AgOTf) then

(8) Piechaczyk, O.; Thoumazet, C.; Jean, Y.; Le Floch, P. *J. Am. Chem. Soc*. **2006**, *128*, 14306–14317.

(9) Mora, G.; Piechaczyk, O.; Houdard, R.; Mézailles, N.; Le Goff, X. F.; Le Floch, P. *Chem. Eur. J*. **2008**, *14*, 10047–10057.

(10) (a) Mézailles, N.; Avarvari, N.; Maigrot, N.; Ricard, L.; Mathey, F.; Le Floch, P.; Cataldo, L.; Berclas, T.; Geoffroy, M. *Angew. Chem., Int. Ed*. **1999**, *38*(21), 3194–3196. (b) Deschamps, E.; Deschamps, B.; Dormieux, J. L.; Ricard, L.; Mézailles, N.; Le Floch, P. *Dalton Trans*. **2006**, 594–602. (c) Heuer, B.; Pope, S. J. A.; Reid, G. *Polyhedron* **2000**, *19*, 743–749. (d) Chan, W.-H.; Mak, T. C. W.; Che, C. M. *Dalton Trans*. **1998**, 2275–2276. (e) Ainscough, E. W.; Brodie, A. M.; Chaplin, A. B.; O'Connor, J. M.; Otter, C. A. *Dalton Trans*. **2006**, 1264–1266. (f) Xu, F.-B.; Li, Q.-S.; Wu, L.-Z.; Leng, X.-B.; Li, Z.-C.; Zeng, X.-S.; Chow, Y. L.; Zhang, Z.-Z. *Organometallics* **2003**, *22*, 633. (g) Poorters, L.; Armspach, D.; Matt, D.; Toupet, L.; Choua, S.; Turek, P. *Chem. Eur. J*. **2007**, 9448–9461. (h) Gibson, A. M.; Reid, G. *J. Chem. Soc., Dalton Trans*. **1996**, 1267.

(11) (a) Ringström, U. *Nature* **1963**, *198*, 981. (b) Ringström, U. *Ark. Fys*. **1964**, *27*, 227–265. (c) Raubenheimer, H. G.; Cronje, J. *Gold, Progress in Chemistry, Biochemistry and Technology*; Schmidbaur, H., Ed.; Wiley: Chischester, 1999; pp 557−632. (d) Pyykkö, P. *Angew. Chem., Int. Ed*. **2004**, *116*, 4512–4557. Pyykkö, P. *Angew. Chem., Int. Ed*. **2004**, *43*, 4412–4456, and references therein.

(12) For a comprehensive review on catalysis by gold complexes or nanoparticles see: (a) Hashmi, A. S. K.; Hutchings, G. J. *Angew. Chem., Int. Ed*. **2006**, *45*, 7896–7936; and references therein. For pertinent references in which Au−H bonds are postulated in catalytic cycles, see for example: (b) Gonzalez-Arellano, C.; Corma, A.; Iglesias, M.; Sanchez, F. *Chem. Commun*. **2005**, 3451–3453. (c) Ito, H.; Takagi, K.; Miyahara, T.; Sawamura, M. *Org. Lett*. **2005**, *7*, 3001–3004.

(13) Tsui, E. Y.; Müller, P.; Sadighi, J. P. *Angew. Chem., Int. Ed*. **2008**, *47*, 8937–8940.

(14) Theoretical calculations carried out at the B3PW91/6-311++G(d, p)//B3PW91 6-31 G(d) level of theory have demonstrated that both conformation of Xantphos-phosphole 1 have nearly the same energy (ΔE = +2.9 kcal/mol) at the same energy. In the first conformation the two phosphorus atom lone pair point towards the plane of symmetry of the ligand (to form a chelate ligand) whereas in the second conformation (+2.9 kcal/mol) one phosphorus atom lone pair points outside the ligand explaining why a monodentate is formed when [Au−Cl] is reacted. The two conformations are in equilibrium through the inversion of one phosphorus atom of one phosphole ring. DFT calculations indicate that the inversion barrier in this type of 1,2,5-tris aryl substituted phosphole is about 16 kcal/mol (RB3PW 6-311++G(d,p) level of theory).

(15) One reviewer of this article suggested that complex **3** could be obtained in pure form by submitting complex **4** to a metathesis with chloride salts. Several attempts were thus made using LiCl as salt in different solvents but each attempt resulted in the formation of **2** and **3** as a mixture.

Scheme 3. Known Au−H Fragments (Homo Metallic Au Complexes) and Our Working Hypothesis

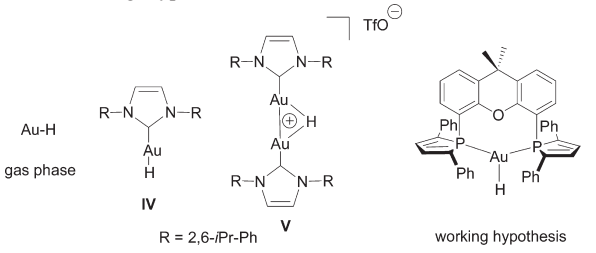

Scheme 4. Synthesis of the Cationic Derivative **4**

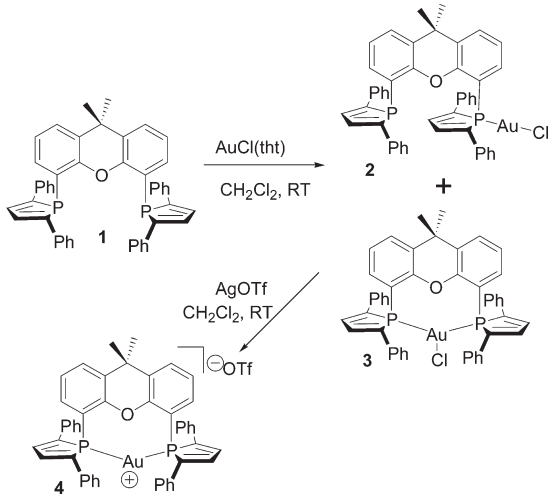

cleanly afforded a single signal in ^{31}P NMR at $\delta = 14.9$ ppm corresponding to complex **4** which was isolated as a very air-stable yellow solid in a quantitative yield (Scheme 4).[15]

The formulation of **4** was established on the basis of ^{1}H and ^{13}C NMR data and elemental analysis. Additional evidence on its formulation was given by an X-ray crystallographic study since single crystals of **4** could be grown by slow diffusion of hexanes (mixture of isomers) into a dichloromethane solution of the complex at room temperature. A view of one molecule of **4** is presented in Figure 1, and the most significant metric parameters are listed in the corresponding legend. Notably, the formation of complex **4** does not require the prior isolation of complexes **2** and **3**. Complex **4** can be straightforwardly obtained by reaction of 1 equiv of the XDPP ligand in dichloromethane at room temperature with 1 equiv of [AuCl(tht)] and 1 equiv of [AgOTf].

Apart from the excepted wide P−Au−P bite angle of 146.97(4)° and the Au−P bond distances (2.301(1) and 2.300(1) Å) which fall in the usual range for this type of complexes, the structure of **4** does not deserve further comments.

Several attempts were made to generate a gold-hydride complex from **4** upon reaction with various hydrides. However, in most cases, whatever the experimental conditions used (solvent, temperature), these reactions essentially led to the formation of colloidal mixtures. The most satisfying result was obtained upon reacting $HSiMe_2Ph$ in tetrahydrofuran (THF) at −78 °C. Reaction of 0.5 equiv of $HSiMe_2Ph$ with **4** cleanly resulted in the formation of a single signal, centered at $\delta = 23.8$ ppm in ^{31}P NMR

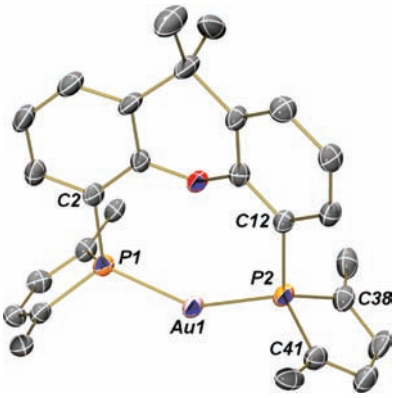

Figure 1. Solid-state structure of the cation of complex **4**. Thermal ellipsoids are set at the 50% probability level. For clarity, phenyl groups of phospholes have been omitted and only the ipso carbon is represented. Selected bond lengths[Å] and angles [deg]: Au(1)−P(1), 2.301(1); Au(1)−P(2), 2.300(1); P(1)−Au(1)−P(2), 146.97(4); P(1)−C(2), 1.820(4); P(2)−C(12), 1.801(5); C(2)−P(1)−Au(1), 108.1(1); C(41)−P(2)−C(38), 93.4(2).

Scheme 5. Synthesis of the Complex **5**

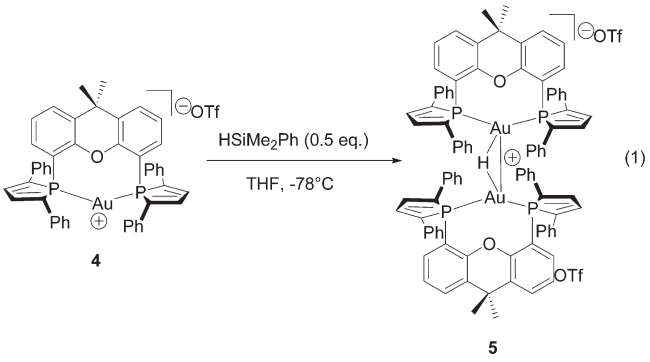

spectroscopy. After washings with diethyl ether and filtration at room temperature, complex **5** was isolated as a very air-stable yellow solid with a 98% yield (Scheme 5).

The structure of **5** could not be simply established on the basis of ^{1}H and ^{13}C NMR data which show no apparent hydride and only exhibit vinylic and aromatic signals of the phosphole and Xantphos units. Note that in the (NHC) Au−H complex **IV**, the hydride resonance was observed at $\delta = 5.11$ ppm in C_6D_6 and 3.38 ppm in CD_2Cl_2. However, the ^{31}P NMR spectrum of **5** shows a very characteristic doublet at 23.8 ppm with a $^{2}J_{HP}$ coupling constant of 54.0 Hz attesting that each phosphorus atom in **5** is coupled with a hydrogen atom. To definitely establish the structure of **5** the hydride was replaced by a deuteride. Reaction of D-$SiMe_2Ph$[16] with complex **4** afforded under the same experimental conditions complex **6** which was isolated after usual workup in 96% yield as a yellow powder (Scheme 6).

Importantly, the ^{2}H NMR spectrum of complex **6** is very characteristic and exhibits a signal which appears as a quintet at $\delta = 7.0$ ppm ($^{2}J_{DP} = 8.4$ Hz) attesting that the deuterium atom is surrounded by four equivalent phosphorus nuclei. Moreover, the $^{31}P\{^{1}H\}$-NMR spectrum shows a pseudo triplet with a coupling constant (J_{DP}) of

(16) Pawlenko S. In *Houben Weyl, Methoden der Organischem Chemie* Müller, E., Bayer, O., Eds.; Thieme Verlag: Stuttgart, NY, 1980; Bd. 13/5, p 90.

Scheme 6. Synthesis of the Deuterated Complex **6**

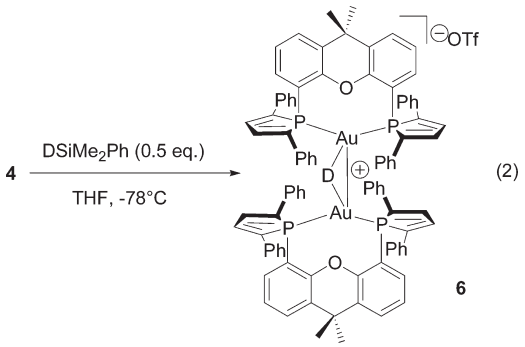

8.4 Hz. The final proof of the similarity of the hydride and the deuteride is given by the ratio of the coupling constants ($J_{HP}/J_{DP} = 54/8.4 = 6.43$) which is essentially equal to the ratio of the gyromagnetic factors ($\gamma^{proton}/\gamma^{deuterium} = 26.753/4.107 = 6.51$). These important informations suggest that complexes **5** and **6** are not monomeric but dinuclear. This chemical shift is not common for hydride species which in most case for others metals are in negative shifts. Note that in the case of the dimer complex **V**, Sadighi et al. reported that the hydride resonates at 0.42 ppm. So far, no studies were undertaken to rationalize the important deshielding observed in the case of our complex **5** but taking into account the important electronic capacities between the two ligands, one may propose that this could result from the strong π-accepting capacity of the XDPP ligand which would increase the acidity of the bridged hydride.

Fortunately, single crystals of complex **5** were obtained by slowly diffusing a mixture of hexanes into a dichloromethane solution of the dimer at room temperature. A view of one molecule of **5**, which presents a C_2 axis, is presented in Figure 2, and the most significant bond lengths and angles are listed in the corresponding legend. A second view of **5** showing the deviation between the two P−Au−P planes and the positioning of the hydrogen atom is presented in Figure 3.

The structure of **5** deserves further comments. First, as expected an hydrido ligand symmetrically binds in μ^2-fashion the two [(XDPP)Au] fragments which are separated by a distance of 2.7542(3) Å. Note that, in the dinuclear complex **V**, the similar separation was found to be significantly shorter at 2.7099(4) Å. A second important piece of data is given by the Au−H bond distance of 1.70(3) Å. Comparison with other species is made difficult since in the corresponding NHC based dimer **V** attempts to locate the gold-bound hydrogen atom in the difference Fourier synthesis failed because of a too-noisy environment around the two gold atoms.[13] In the case of the complex NHC Au−H **IV** the hydrogen atom was positioned on the basis of a second residual density maximum.[13] Furthermore, no direct comparison can be drawn with [AuHM] complexes since in these latter the Au−H bond lengths vary considerably. Thus, in the $[(PPh_3)_3(CO)Ru(\mu^2\text{-}H)_2Au(PPh_3)]^+$ complex the Au−H

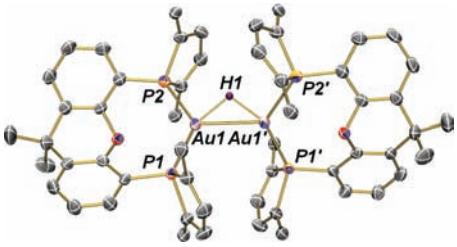

Figure 2. Solid-state structure of the cation of complex **5**. Thermal ellipsoids are set at the 50% probability level. For clarity, phenyl groups of phospholes have been omitted and only the ipso carbon is represented. Complex **5** presents a C_2 axis (H(1) and the middle of Au(1)−Au(1′) bond are on the axis). Selected bond lengths [Å] and angles [deg]: Au(1)−P(1), 2.308(1); Au(1)−P(2), 2.446(1); Au(1)−Au(1′), 2.7542(3); Au(1)−H(1), 1.70(3); P(1)−Au(1)−P(2), 124.77(3); P(2)−Au(1)−Au(1′), 117.24(2); P(1)−Au(1)−Au(1′), 117.08(2); P(1)−Au(1)−H(1), 144.9(8); P(2)−Au(1)−H(1), 89(1); Au(1′)−Au(1)−H(1), 36(1); P(2)−Au(1)−Au(1′)−P(2′), 82.63(2); P(1)−Au(1)−Au(1′)−P(1′), 61.82(2); P(1)−Au(1)−Au(1′)−P(2′), 72.23(2).

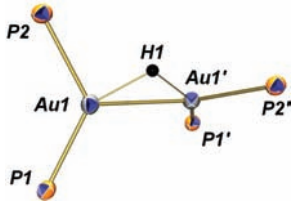

Figure 3. Other view of **5** restricted to the $[Au_2P_4H]^+$ core showing the deviation between the two P−Au−P planes.

bond is particularly short at 1.616 Å,[17] whereas it is very long at 1.976 Å in the $[(dppm)_2Ru(\mu^2\text{-}H)_2Au(PPh_3)]^+$ complex[18] (dppm = bis-diphenylhosphinomethane).[19] Another important observation concerns the respective arrangement of the two $[(XDPP)Au]^+$ fragments. As can be easily seen in Figure 3, the two fragments are not coplanar and adopt a twist angle. Most probably, this deviation results from the steric congestion due to the diphenylphosphole substituents rather than to electronic effects. Undoubtedly, the most intriguing structural feature arises from the P−Au bonds which are markedly different. Thus the P(1)−Au bond lengths (2.308(1)Å) are found to be shorter than the P(2)−Au bonds (2.446(1)Å) in each $[Au(XDPP)]^+$ unit. This result is quite unexpected if one takes into account that the two P1 atoms are nearly *trans* to the hydrido ligand which is well-known to display a strong *trans* influence.

The reactivity of dimer **5** was briefly explored. A first interesting remark concerns its stability in solution. Though poorly soluble in common organic solvents, such as hexanes, toluene, and ethers, **5** is fairly soluble in chlorinated solvents but decomposes overnight in dichloromethane to afford colloidal gold and a new complex **7** whose structure could be straightforwardly established on the basis of the ^{31}P NMR spectrum. Indeed, the presence of a triplet at $\delta = 40.7$ ppm with $^2J_{PP} = 196$ Hz, a doublet at $\delta = 16$ ppm with $^2J_{PP} = 196$ Hz and of a singlet at −12.4 pm is very characteristic of a

(17) Alexander, B. D.; Gomez-Sal, M. P.; Gannon, P. R.; Blaine, C. A.; Boyle, P. D.; Mueting, A. M.; Pignolet, L. H. *Inorg. Chem.* **1988**, *27*, 3301.
(18) Alexander, B. D.; Johnson, B. J.; Johnson, S. M.; Boyle, P. D.; Kann, N. C.; Mueting, A. M.; Pignolet, L. H. *Inorg. Chem.* **1987**, *26*, 3506.
(19) For a selection Au−H bond distances in [M−H−Au]+ complexes, see: (a) Lehner, H.; Matt, D.; Pregosin, P. S.; Venanzi, L. M.; Albinati, A. *J. Am. Chem. Soc.* **1982**, *104*, 6825–6827. (b) Albinati, A.; Chaloupka, S.; Currao, A.; Klooster, W. T.; Koetzle, T. F.; Nesper, R.; Vananzi, L. M. *Inorg. Chim. Acta* **2000**, *300*−*302*, 903–911. (c) Alexander, B. D.; Johnson, B. J.; Johnson, S. M.; Casalnuovo, A. L.; Pignolet, L. H. *J. Am. Chem. Soc.* **1986**, *108*, 4409–4417.

Scheme 7. Synthesis of the Complex **7**

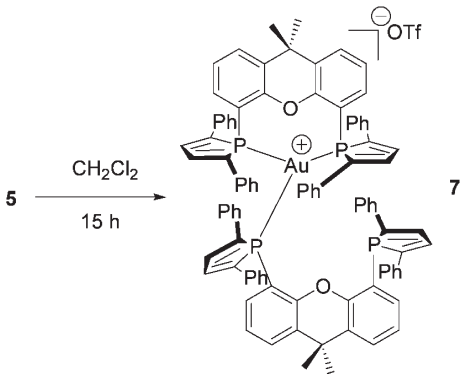

tricoordinated mononuclear Au(I) complex (Scheme 7). This assumption was further confirmed by detailed analyses of the ^{1}H and ^{13}C NMR spectra as well as by elemental analysis.

Definitive evidence was given by an X-ray crystal structure analysis of **7**, single crystals being obtained by diffusion of a solution of hexanes into a dichloromethane solution of the complex. A view of one molecule of **7** is presented in Figure 4, and the most relevant bond distances and angles are listed in the corresponding legend.

This structure does not deserve special comment except for the P(1)−Au(1)−P(2) bond angle. Indeed, it is significantly smaller than in complex **4** (120.58(3) in **7** versus 146.97(4) in **4**), reflecting here again a significant flexibility of the XDPP bite angle. One may also note the different coordination mode from that of the Xantphos ligand which can form the homoleptic tetracoordinated cationic 18 VE complex.[20]

In their article, Sadighi et al. reported that their dinuclear $[Au_2H]^+$ complex could serve as a source of the monomeric species [Au−H] upon reaction with NaO*t*Bu. Unfortunately, addition of KO*t*Bu led to a rapid decomposition of complex **5**, and careful monitoring of the progress of the reaction by ^{31}P NMR did not allow to establish the formation of any [(XDPP)Au−H] complex.

Density Functional Theory (DFT) Calculations. To shed some light on the electronic structure of dimer **5**, theoretical calculations were carried out within the framework of DFT (see Experimental Section for further details). Calculations were carried out on the whole structure including all substituents except the two methyl groups of the Xantphos backbone which were replaced by hydrogen atoms. The geometry of the $[(XDPP)_2Au_2(\mu^2\text{-}H)]^+$ dimer **5** was optimized without any symmetry constraint.[21] A view of the optimized structure is reported in Figure 5, and the most significant metric parameters are listed in the corresponding legend. On the whole, the main features of the experimental structure were properly reproduced by these calculations, the hydride ligand bridging the two metal centers with Au−H = 1.76 Å

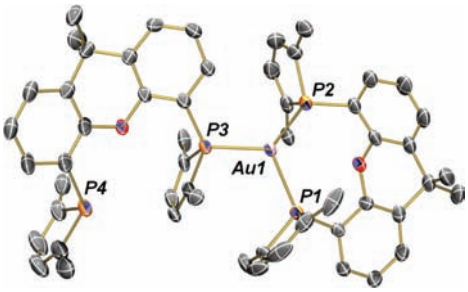

Figure 4. Solid-state structure of the cation of complex **7**. Thermal ellipsoids are set at the 50% probability level. For clarity, phenyl groups of phospholes have been omitted and only the ipso carbon is represented. Selected bond lengths [Å] and angles [deg]: Au(1)−P(1), 2.37(1); Au(1)−P(3), 2.37(1); Au(1)−P(2), 2.42(1); P(1)−Au(1)−P(3), 125.7(5); P(1)−Au(1)−P(2), 120.6(5); P(3)−Au(1)−P(2), 112.8(5).

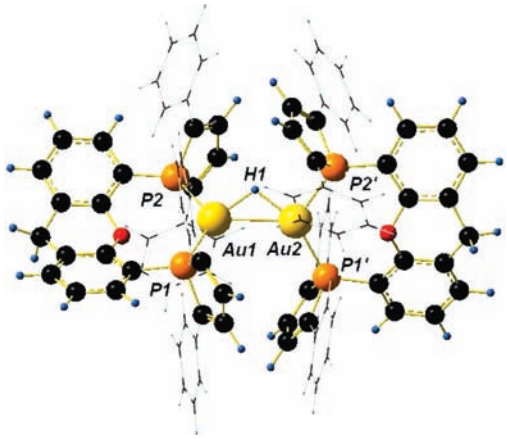

Figure 5. View of the optimized structure of complex **5**. The phenyl groups on phosphole units have been drawn in wireframe for sake of clarity. Selected bond lengths[Å] and angles [deg]: Au(1)−P(1), 2.357, Au(1)−P(2) 2.517, Au(1)−Au(2) 2.824, Au(1)−H(1) 1.763, Au(2)−H(1) 1.758, P(1)−Au(1)−P(2) 121.2, P(2)−Au(1)−Au(2) 119.1, P(1)−Au(1)−Au(2) 118.5, P(1)−Au(1)−H(1) 89.9, P(2)−Au(1)−H(1) 89.9, and Au(2)−Au(1)−H(1) 36.7.

(exp.: 1.70 (3) Å) and the twisted arrangement of the two XDPP ligands (see P−Au−Au−P dihedral angles). The bond distances around the metal centers were overestimated at most by 0.07 Å. Noteworthy, like in the experimental structure, the two Au−P distances associated with a XDPP ligand differ by 0.16 Å (difference of 0.14 Å in the experimental structure). Surprisingly, the longest Au−P distances are those approximately *cis* with the hydride ligand. Finally a mean deviation of 2° was found for the bond angles. Berger et al.,[22] in a recent theoretical study on $[Au_2H]^+$, obtained an Au−Au bond distance of 2.60 Å and an Au−H bond distance of 1.69 Å. These distances are much shorter than the Au−Au distance of 2.824 Å and Au−H distance of 1.763 Å calculated here for complex **5**. The differences are obviously due to the presence of the π-acceptor ligands on the $[Au_2H]^+$ fragment in the real system.

To understand the way the hydride ligand binds the two metal centers, a molecular orbital analysis was performed on the whole complex and on various fragments. The $[(XDPP)_2Au_2(\mu^2\text{-}H)]^+$ complex can be seen as resulting from the interaction of an hydride H^- with the

(20) (a) Pintado-Alba, A.; de la Riva, H.; Nieuwhuyzen, M.; Bautista, D.; Raithby, P. R.; Sparkes, H. A.; Teat, S. J.; Lopez-de-Luzuriaga, J. M.; Lagunas, M. C. *Dalton Trans*. **2004**, 3459. (b) Deak, A.; Megyes, T.; Tarkanyi, G.; Kiraly, P.; Biczok, L.; Palinkas, G.; Stang, P. J. *J. Am. Chem. Soc*. **2006**, *128*, 12668–12670.

(21) Despite many attempts, we could not avoid the presence of one very small imaginary frequency at −9.7650 corresponding mainly to the rotation of a phenyl group on one phosphole part of the ligand.

(22) Berger, R. J. F. *Z. Naturforsch*. **2009**, *64b*, 388–394.

Scheme 8. Frontier Orbitals of the Bent $[L_2Au]^+$ Monomer B (Left-Hand Side) and MOs of the $[L_2AuAuL_2]^{2+}$ Dicationic Dimer A (Right-hand Side) Relevant for the Interaction Diagram Reported on Scheme 6

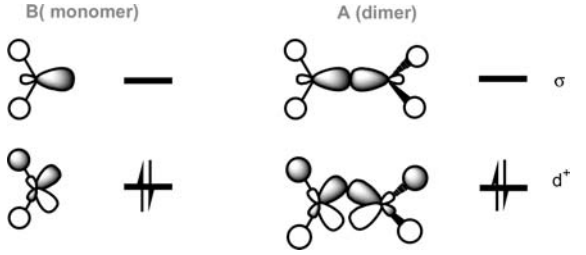

Scheme 9. Three-Orbital Interaction Diagram Explaining the Interaction between H^- and the $[L_2AuAuL_2]^{2+}$ Fragment and the Shape of the HOMO

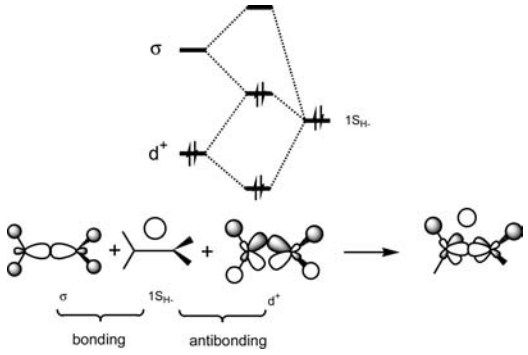

$[(XDPP)_2Au_2]^{2+}$ fragment (**A**). This dicationic dimer **A** can in turn be decomposed into two identical mononuclear $[(XDPP)Au]^+$ fragments (**B**) which are d^{10}-ML_2 complexes adopting a bent geometry. The lowest unoccupied molecular orbital (LUMO; mainly s-p hybrid orbital on the metal center with a contribution on the ligands) and the highest occupied d orbital of **B** are schematically pictured in Scheme 8.[23] Thus the LUMO of dimer **A** results from the bonding combination of the LUMOs of the **B** fragments (see Scheme 8). This molecular orbital (MO, σ) is widely developed between the two metal centers, and its pseudo-cylindrical symmetry around the Au−Au axis allows an interaction with the 1s orbital of the incoming hydride (stabilizing two-orbital two-electron interaction). As can be seen, the bonding combination of the occupied d orbitals on fragments **B**, yields the MO d^+ of dimer **A** (Scheme 8) which also has the appropriate symmetry to interact $1s_{H-}$ through a destabilizing two-orbital four-electron interaction.

On the whole, a three-orbital four-electron interaction scheme has to be considered (Scheme 9). The shape of the highest occupied molecular orbital (HOMO) of the whole complex thus results from the combination of a bonding interaction between $1s_{H-}$ and σ and from an antibonding interaction between $1s_{H-}$ and d^+.[24] Consequently, according to the way the σ and d^+ fragment orbitals participate in the HOMO, the antibonding contributions on P ligands are predicted to vanish on the ligands *trans* to the hydride and to add on the *cis* ligands.

(23) Jean Y. *Molecular Orbitals of Transition Metal Complexes*; Oxford University Press: London, 2005; pp 83−84.

(24) Jean Y.; Volatron, F. *An Introduction to Molecular Orbitals*; Oxford University Press: New York, 1996; Chapter 6.

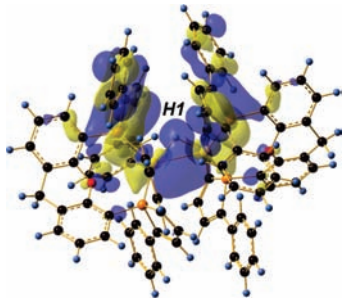

Figure 6. HOMO of complex **5** as given by DFT calculations.

Table 1. Bond Distances (Å) and Angles (deg) of the Complex **5** in the Crystal Structure[a] and As Calculated by DFT

bond/angle	exp.	DFT
Au(1)−P(1)	2.308(1)	2.357
Au(1)−P(2)	2.446(1)	2.517
Au(1)−Au(2)	2.7542(3)	2.824
Au(1)−H(1)	1.70(3)	1.763
Au(2)−H(1)	1.70(3)	1.758
P(1)−Au(1)−P(2)	124.77(3)	121.2
P(2)−Au(1)−Au(2)	117.24(2)	119.1
P(1)−Au(1)−Au(2)	117.08(2)	118.5
P(1)−Au(1)−H(1)	144.9(8)	147.3
P(2)−Au(1)−H(1)	89(1)	89.9
Au(2)−Au(1)−H(1)	36(1)	36.7
P(2)−Au(1)−Au(2)−P(1′)	72.23(2)	69.8
P(2)−Au(1)−Au(2)−P(2′)	82.63(2)	82.6
P(1)−Au(1)−Au(2)−P(1′)	61.82(2)	57.5
P(1)−Au(1)−Au(2)−P(2′)	72.23(2)	70.3

[a] For a better comparison of X-ray and theoretical data, Au(1′) in the X-ray data was renamed as Au(2) in the table.

The actual shape of the HOMO pictured in Figure 6 confirms this analysis. There is a three-center (Au−H−Au) bonding interaction resulting from the bonding mixing of $1s_{H-}$ and σ fragment orbitals. Small antibonding Au−H interactions also appear which involve a d component on the metal centers (antibonding mixing between $1s_{H-}$ and d^+). Finally antibonding components on the P ligands appear only on the ligands *cis* to the hydride. This nicely rationalizes the lengthening of the two Au−P bonds located approximately *cis* to the hydride (Table 1), an unexpected result with respect to the usual *trans* influence exerted by a hydride ligand.

Conclusion

In conclusion we have shown that the XDPP ligand belongs to the class of rare bidentate ligands that allow the stabilization of 14 VE chelate gold cationic complexes of general formula $[Au(L_2)]^+$. Though formation of the neutral 16 VE gold-hydride complex [Au(XDPP)(H)] could not be observed, a cationic dimetallic gold hydride complex $[Au_2(XDPPP)_2(H)]^+$, formally resulting from the stabilization of the gold hydride complex by the $[Au(XDPP)]^+$ complex could be synthesized and successfully structurally and spectroscopically characterized. DFT calculations carried out on the real model establish that this dimetallic complex can be viewed as the interaction of H^- with the dimetallic dicationic $[Au_2(XDPPP)_2]^{2+}$ fragment. Importantly, a detailed MO analysis reveals that bonding between H and Au in $[Au_2(XDPPP)_2(H)]^+$ does not simply results from the two orbital

interaction between H^- and an empty σ Au−Au orbital. A four electron three orbital interaction diagram, also involving the participation of a filled d orbital at gold, is involved. This particular electronic situation allows to nicely rationalize the difference observed between P−Au bonds. Further studies will now focus on the reactivity of this new class of cationic XDPP gold complexes and their potential use as catalysts.

Experimental Section

Synthesis. All reactions were routinely performed under an inert atmosphere of argon or nitrogen using Schlenk and glovebox techniques and dry deoxygenated solvents. Dry hexanes and THF were obtained by distillation from Na/benzophenone. Dry dichloromethane was distilled on P_2O_5. Nuclear magnetic resonance spectra were recorded on a Bruker AC-300 SY spectrometer operating at 300.0 MHz for ^{1}H, 75.5 MHz for ^{13}C, and 121.5 MHz for ^{31}P. Solvent peaks are used as internal reference relative to Me_4Si for ^{1}H and ^{13}C chemical shifts (ppm); ^{31}P chemical shifts are relative to an 85% H_3PO_4 external reference. Coupling constants are given in hertz. The following abbreviations are used: s, singlet; d, doublet; t, triplet; m, multiplet; v, virtual; p, pseudo. XDPP **1** was prepared as previously reported. [AuCl(tht)] was prepared according to established procedure.[25] Silver trifluoromethanesulfonate and the silane $HSiMe_2Ph$ were obtained from commercial suppliers and were used as received. The deuterated silane $DSiMe_2Ph$ was prepared according to established procedure.[26] Elemental analyses were performed by the "Service d'analyse du CNRS", at Gif sur Yvette, France.

Synthesis of Complex 4 [Au(XDPP)][OTf]. To a solution of [AuCl(tht)]] (94.5 mg, 0.29 mmol) in dichloromethane (3 mL) was added at room temperature the ligand **1** XDPP (200 mg, 0.29 mmol) . The solution was stirred 5 min. Completion of the reaction was confirmed by ^{31}P NMR. Silver triflate salt (75.7 mg, 0.29 mmol) was then added to the solution at room temperature. The mixture was stirred 15 min, filtered, and concentrated. The corresponding solid was washed with hexanes. The solvent was removed to afford a yellow solid **4** (295 mg, 98%). $^{31}P\{^1H\}$ NMR (CD_2Cl_2): δ 14.9 (s). ^{1}H NMR (CD_2Cl_2): δ1.56 (s, 6H, $CH_{3xanthene}$), 6.99−7.05 (m, 2H, $CH_{xanthene}$), 7.1 (t, 2H, $CH_{xanthene}$), 7.14−7.27 (m, 12H, $H_{meta/para\ phenyl}$), 7.6 (d, 4H, J_{HP} = 27 Hz, $H_{\beta\ phosphole}$), 7.51−7.57 (m, 8H, $H_{ortho\ phenyl}$), 7.58−7.62 (m, 2H, $CH_{xanthene}$).^{13}C NMR (CD_2Cl_2): δ 29.7 (s, $CH_{3xanthene}$), 35.7 (s, $C(CH_3)_{2\ xanthene}$), 110.1 (vt, ΣJ = 46.4 Hz, $C_{xanthene}P$), 125.4(vt, ΣJ = 8 Hz, $CH_{aromatic}$), 125.3 (vt, ΣJ = 8 Hz, $CH_{aromatic}$), 128.4 (s, $CH_{aromatic}$), 128.6(s, $CH_{aromatic}$), 129.2 (s, $CH_{aromatic}$), 130.0 (s, $CH_{aromatic}$), 131.9 (vt, ΣJ = 14.8 Hz, $C_{aromatic}$), 135.3 (vt, ΣJ = 5 Hz, $C_{aromatic}$), 135.6 (vt, ΣJ = 18 Hz, $C_{\beta\ phosphole}$), 144.3 (vt, ΣJ = 48 Hz, $C_{\alpha\ phosphole}$), 154.6 (vt, ΣJ = 11 Hz, CO). Anal. Calcd for $C_{48}H_{36}AuF_3O_4P_2S$: C, 56.26; H, 3.54. Found: C, 56.20; H, 3.57.

Synthesis of Complex 5 [(XDPP)Au−H−Au(XDPP)][OTf]. To a solution of the complex **4** (139 mg, 0.13 mmol) in THF (2 mL) was added at −78 °C the silane $HSiMe_2Ph$ (10.5 μL, 0.065 mmol). Completion of the reaction was confirmed by ^{31}P NMR. The mixture was allowed to warm to room temperature. The title compound, which precipitated, was then filtered under nitrogen. The corresponding solid was washed with diethylether. The solvent was removed to afford a yellow-brown solid **5** (180 mg, 70%). $^{31}P\{^1H\}$ NMR (CD_2Cl_2): δ 23.8 (s). ^{1}H NMR (CD_2Cl_2): δ 1.56 (s, 12H, $CH_{3xanthene}$), 6.35 (m, 8H, ΣJ_{HP} = 23 Hz, $H_{\beta\ phosphole}$), 6.75 (m,4H, $CH_{xanthene}$), 6.95 (t, 4H, J = 8.4 Hz, $CH_{xanthene}$), 7.05−7.25 (m, 32H, $H_{meta/ortho\ phenyl}$), 7.36 (m, 8H, $H_{para\ phenyl}$), 7.42−7.50 (dd, 4H, $CH_{xanthene}$). ^{13}C NMR (CD_2Cl_2): δ 31.3 (s, $CH_{3xanthene}$), 39.34 (s, $C(CH_3)_{2xanthene}$), 115.21 (m,35.6 Hz, $C_{xanthene}P$), 128.24 (s, $CH_{aromatic}$), 129.4 (s, $CH_{aromatic}$), 131.18 (s, $CH_{aromatic}$), 131.98 (s, $CH_{aromatic}$), 132.18 (s,$CH_{aromatic}$), 134.19 (s, $CH_{aromatic}$), 137.01 (m, ΣJ = 15 Hz, $C_{aromatic}$), 137.81 (m, ΣJ = 15 Hz, $C_{\beta\ phosphole}$), 138.19 (m, ΣJ = 5 Hz, $C_{aromatic}$)149.63 (m, ΣJ = 44 Hz, $C_{\alpha\ phosphole}$), 159.27 (m, ΣJ = 13 Hz, CO). Anal. Calcd for $C_{95}H_{73}Au_2F_3O_5P_4S$: C, 60.01; H, 3.87. Found: C, 60.05; H, 3.90.

Synthesis of Complex 6 [(XDPP)Au-D-Au(XDPP)][OTf]. To a solution of the complex **4** (152 mg, 0.15 mmol) in THF (2 mL) was added at −78 °C the silane $DSiMe_2Ph$ (11.6 μL, 0.075 mmol). Completion of the reaction was confirmed by ^{31}P NMR. The mixture was allowed to warm to room temperature. The title compound, which precipitated, was then filtered under nitrogen. The corresponding solid was washed with diethylether. The solvent was removed to afford a yellow-brown solid **6** (190 mg, 67%). $^{31}P\{^1H\}$ NMR (CD_2Cl_2): δ 23.8 (pt, J_{DP} = 8.4 Hz). ^{1}H NMR (CD_2Cl_2): δ 1.56 (s, 12H, $CH_{3xanthene}$), 6.35 (m, 8H, ΣJ_{HP} = 23 Hz, $H_{\beta\ phosphole}$), 6.75 (m,4H, $CH_{xanthene}$), 6.95 (t, 4H, J = 8.4 Hz, $CH_{xanthene}$), 7.05−7.25 (m, 32H, $H_{meta/ortho\ phenyl}$), 7.36 (m, 8H, $H_{para\ phenyl}$), 7.42−7.50 (dd, 4H, $CH_{xanthene}$). ^{2}D-NMR (CH_2Cl_2): δ 7.0 (q, J_{DP} = 8.4 Hz). ^{13}C NMR (CD_2Cl_2): δ 31.3 (s, $CH_{3xanthene}$), 39.34 (s, $C(CH_3)_{2xanthene}$), 115.21 (m,35.6 Hz, $C_{xanthene}P$), 128.24 (s, $CH_{aromatic}$), 129.4 (s, $CH_{aromatic}$), 131.18 (s, $CH_{aromatic}$), 131.98 (s, $CH_{aromatic}$), 132.18 (s, $CH_{aromatic}$), 134.19 (s, $CH_{aromatic}$), 137.01 (m, ΣJ = 15 Hz, $C_{aromatic}$), 137.81 (m, ΣJ = 15 Hz, $C_{\beta\ phosphole}$), 138.19 (m, ΣJ = 5 Hz, $C_{aromatic}$)149.63 (m, ΣJ = 44 Hz, $C_{\alpha\ phosphole}$), 159.27 (m, ΣJ = 13 Hz, CO). Anal. Calcd for $C_{95}H_{72}DAu_2F_3O_5P_4S$: C, 59.97; H, 3.92. Found: C, 60.04; H, 3.89.

Synthesis of Complex 7 [Au(XDPP)$_2$][OTf]. A solution of the complex **5** (30.1 mg, 0.029 mmol) in dichloromethane (1 mL) was stirred overnight. Completion of the reaction was confirmed by ^{31}P NMR. The solvent was removed to afford a yellow solid **7** (25 mg, 93%). $^{31}P\{^1H\}$ NMR (CD_2Cl_2): δ −12.4 (s), 16 (d), 40.7 (t). ^{1}H NMR (CD_2Cl_2): δ 1.19 (s, 6H, $CH_{3xanthene}$), 1.41 (s, 6H, $CH_{3xanthene}$), 6.28−6.65 (m, 10H, $H_{aromatic}$), 6.66−7.18 (m, 32H, $H_{aromatic}$), 7.2−7.5 (m, 14H, $H_{aromatic}$), 7.51−7.80 (m, 4H, $H_{aromatic}$). ^{13}C NMR (CD_2Cl_2): δ 26.9 (s,$CH_{3xanthene}$), 30.4 (s,$CH_{3xanthene}$), 33.8 (s, $C(CH_3)_{2xanthene}$), 35.63 (s,$C(CH_3)_{2xanthene}$), 110.70 (m, ΣJ = 49.7 Hz,$C_{xanthene}P$), 112.92 (s, ΣJ = 48.2 Hz, $C_{xanthene}P$), 117.18 (d, J = 13.7 Hz, $C_{xanthene}P$), 122.52 (d, J = 18.8 Hz, $CH_{aromatic}$), 123.58 (s, $CH_{aromatic}$), 124.73 (d, ΣJ = 8.1 Hz, $CH_{aromatic}$), 124.84 (d, J = 8 Hz, $CH_{aromatic}$), 125.02 (m, ΣJ = 9.6 Hz, $CH_{aromatic}$), 125.42 (vt, ΣJ = 8.6 Hz, $CH_{aromatic}$), 126.23 (s, $CH_{aromatic}$), 127.13 (s, $CH_{aromatic}$), 127.87 (s, $CH_{aromatic}$), 127.93 (s, $CH_{aromatic}$), 128.51 (s, $CH_{aromatic}$), 129.04 (d, ΣJ = 5.1 Hz, $CH_{aromatic}$), 130.45 (d, ΣJ = 5.1 Hz, $C_{aromatic}$), 130.71 (d, J = 11.6 Hz, $CH_{aromatic}$), 131.10 (m, ΣJ = 6 Hz, $CH_{aromatic}$), 131.31 (d, J = 3.8 Hz, $CH_{aromatic}$), 131.4 (d, J = 3.5 Hz, $CH_{aromatic}$),

(25) Uson, R.; Laguna, A. In *Organometallics Syntheses*; King, R. B., Eisch, J., Eds.; Elsevier Science, Amsterdam, 1986; Vol. *3* p 324.

(26) Pawlenko, S. *Houben Weyl, Methoden der Organischem Chemie*; Müller, E., Bayer, O., Eds.; Thieme Verlag, Stuttgart, NY 1980; Bd. 13/5, p. 90.

(27) Frisch, M. J.; Trucks, G. W.; Schlegel, H. B.; Scuseria, G. E.; Robb, M. A.; Cheeseman, J. R.; Montgomery, J. A., Jr.; Vreven, T.; Kudin, K. N.; Burant, J. C.; Millam, J. M.; Iyengar, S. S.; Tomasi, J.; Barone, V.; Mennucci, B.; Cossi, M.; Scalmani, G.; Rega, N.; Petersson, G. A.; Nakatsuji, H.; Hada, M.; Ehara, M.; Toyota, K.; Fukuda, R.; Hasegawa, J.; Ishida, M.; Nakajima, T.; Honda, Y.; Kitao, O.; Nakai, H.; Klene, M.; Li, X.; Knox, J. E.; Hratchian, H. P.; Cross, J. B.; Bakken, V.; Adamo, C.; Jaramillo, J.; Gomperts, R.; Stratmann, R. E.; Yazyev, O.; Austin, A. J.; Cammi, R.; Pomelli, C.; Ochterski, J. W.; Ayala, P. Y.; Morokuma, K.; Voth, G. A.; Salvador, P.; Dannenberg, J. J.; Zakrzewski, V. G.; Dapprich, S.; Daniels, A. D.; Strain, M. C.; Farkas, O.; Malick, D. K.; Rabuck, A. D.; Raghavachari, K.; Foresman, J. B.; Ortiz, J. V.; Cui, Q.; Baboul, A. G.; Clifford, S.; Cioslowski, J.; Stefanov, B. B.; Liu, G.; Liashenko, A.; Piskorz, P.; Komaromi, I.; Martin, R. L.; Fox, D. J.; Keith, T.; Al-Laham, M. A.; Peng, C. Y.; Nanayakkara, A.; Challacombe, M.; Gill, P. M. W.; Johnson, B.; Chen, W.; Wong, M. W.; Gonzalez, C.; Pople, J. A. *Gaussian 03*, revision C.02; Gaussian, Inc.: Wallingford, CT, 2004.

Table 2. Crystallographic Data for Complexes **4**, **5**, and **7**

	4	**5**	**7**
empirical formula	$C_{47}H_{36}AuOP_2,CF_3O_3S, 2CH_2Cl_2$	$C_{94}H_{73}Au_2O_2P_4,CF_3O_3S$	$C_{94}H_{72}AuO_2P_4,CF_3O_3S, 2CH_2Cl_2$
M_r	1194.59	1901.41	1873.28
crystal system	triclinic	orthorhombic	monoclinic
space group	$P\bar{1}$	*Pbcn*	$P2_1/c$
a [Å]	16.447(1)	20.828(1)	18.430(1)
b [Å]	16.986(1)	15.631(1)	18.044(1)
c [Å]	17.884(1)	23.608(1)	31.243(1)
α [deg]	95.103(1)	90.00	90.00
β [deg]	101.052(1)	90.00	124.869(1)
γ [deg]	99.753(1)	90.00	90.00
volume [Å]	4794.5(5)	7685.9(7)	8524.5(7)
Z	4	4	4
ρ_{calcd} [g.cm^{-3}]	1.655	1.643	1.460
μ [mm^{-1}]	3.458	3.988	2.011
crystal size [mm]	0.28*0.24*0.20	0.50*0.12*0.12	0.24*0.20*0.06
reflections collected	51145	75831	67381
unique reflections (R_{int})	27699 (0.0448)	11204 (0.0573)	24828 (0.0506)
R [$F > 4\sigma(F)$]	0.0481	0.0316	0.0447
R_{wF} (all F^2)	0.1370	0.0849	0.1372
GoF	0.993	1.010	0.967

131.97 (vt, $\Sigma J = 15.2$ Hz, $C_{aromatic}$), 132.16 (s, $C_{aromatic}$), 134.25 (d, $J = 16.8$ Hz, $C_{aromatic}$), 134.52 (vt, $\Sigma J = 6$ Hz, $C_{aromatic}$), 135.16 (m, $\Sigma J = 24.9$ Hz, $C_{\beta\ phosphole}$), 136.40 (d, $J = 46$ Hz, $C_{\alpha\ phospole}$), 138.47(d, $J = 35.7$ Hz, $CH_{aromatic}$), 145.67 (vt, $\Sigma J = 43.9$ Hz, $C_{\alpha\ phosphole}$), 152.17 (d, $\Sigma J = 4.3$ Hz, $C_{\alpha\ phospole}$), 152.64 (d, $\Sigma J = 8$ Hz, CO), 152.73 (s, CO), 155.08 (vt, $\Sigma J = 11.6$ Hz, CO). Anal. Calcd for $C_{95}H_{72}AuF_3O_5P_4S$: C, 66.98; H, 4.26. Found: C, 67.04; H, 4.30.

Computational Details. Calculations were performed with the Gaussian 03 series of program.[27] DFT[28,29] was applied for the complex $[(XDPP)_2Au_2(\mu^2\text{-}H)]^+$ (in which the methyl substituents on the xanthenes backbone were replaced by hydrogen atoms) with the B3PW91 functional.[30,31] A quasi-relativistic effective core potential operator was used to represent the 60 innermost electrons of the gold atoms.[32] The basis set for the metal was the quadruple-ζ basis set associated to the pseudopotential[33] (Def2-QZVP calculations). 6-31G+* basis set was used for the atoms directly bonded to the metal centers (P atoms and the bridging hydride).[34] 3-21G* was used for the phosphole cycles[35] and 3-21G for the phenyl groups carried by the phosphole cycles and for the xanthenes backbone.[36] The minimum energy was characterized by vibration frequencies calculations.

X-ray Crystallography for Complexes 4, 5, 7. Yellow blocks of **4**, brown needles of **5** and yellow plates of **7** crystallized by slow diffusion of hexanes into a saturated dichloromethane solution of respectively **4**, **5**, and **7**. Data were collected on a Nonius Kappa CCD diffractometer using a Mo Kα ($\lambda = 0.71073$ Å) X-ray source and a graphite monochromator at 150 K. Experimental details are described in Table 2. The crystal structures were solved using SIR 97[37] and SHELXL97.[38] Oak Ridge Thermal Ellipsoid Plot (ORTEP) drawings were made using ORTEP III for Windows.[39] Crystallographic data can be obtained free of charge at www.ccdc.cam.ac.uk/conts/retrieving.html [or from the Cambridge Crystallographic Data Center, 12 Union Road, Cambridge CB21EZ, U.K.; fax: (int) +44−1223/336−033 ; e-mail: deposit@ccdc.cam.ac.uk] with the deposition numbers CCDC 731892−731894, respectively, for **4**, **5**, and **7**.

Acknowledgment. The CNRS, the Ecole Polytechnique, and the IDRIS (for computer time, Project No. 090616) are thanked for supporting this work.

Supporting Information Available: Computational details, computed Cartesian coordinates, energies, three lower frequencies of all theoretical structures, an X-ray structure and tables giving crystallographic data for **4**, **5**, and **7** (including atomic coordinates, bond lengths and angles, and anisotropic displacement parameters). This material is available free of charge via the Internet at http://pubs.acs.org.

(28) Ziegler, T. *Chem. Rev.* **1991**, *91*, 651–667.
(29) Parr, R. G.; Yang, W. *DFT*; Oxford University Press: Oxford, U.K., 1989.
(30) Becke, A. D. *J. Chem. Phys.* **1993**, *98*, 5648–5652.
(31) Perdew, J. P.; Wang, Y. *Phys. Rev. B* **1992**, *45*, 13244–13249.
(32) Andrae, D.; Haüssermann, U.; Dolg, M.; Stoll, H.; Preuss, H. *Theor. Chim. Acta* **1990**, *77*, 123–141.
(33) Weigend, F.; Ahlrichs, R. *Phys. Chem. Chem. Phys.* **2005**, *7*, 3297–3305.
(34) Clark, T.; Chandrasekhar, J.; Spitznagel, G. W.; Von Ragué Scleyer, P. *J. Comput. Chem.* **1983**, *4*, 294.
(35) Pietro, W. J.; Francl, M. M.; Hehre, W. J.; Defrees, D. J.; Pople, J. A.; Binkley, S. *J. Am. Chem. Soc.* **1982**, *104*, 5039–5048.
(36) Binkley, S.; Pople, J. A.; Hehre, W. J. *J. Am. Chem. Soc.* **1980**, *102*, 939–947.
(37) Altomare, A.; Burla, M. C.; Camalli, M.; Cascarano, G.; Giacovazzo, C.; Guagliardi, A.; Moliterni, A. G. G.; Polidori, G.; Spagna, R. *SIR97, an integrated package of computer programs for the solution and refinement of crystal structures using single-crystal data.*
(38) Sheldrick, G. M., *SHELXL-97*; Universität Göttingen: Göttingen, Germany, 1997.
(39) Farrugia, L. J., *ORTEP-3*; Department of Chemistry, University of Glasgow: Glasgow, Scotland, U.K., 2001.